# Effect of Solute−Solvent Compatibility on Total Luminescence Spectra of Perylene in Shpol'skii Matrixes at Liquid Helium Temperature

**Krystyna Palewska,* Józef Lipiński, Tomasz Misiaszek, and Juliusz Sworakowski**

*Institute of Physical and Theoretical Chemistry, Technical University of Wrocław, Wybrzeże Wyspiańskiego 27, PL-50-370 Wrocław, Poland*

*Received: February 21, 2002*

Fluorescence excitation and emission spectra of perylene in *n*-alkane Shpol'skii matrixes have been studied at liquid helium temperature. The presence of a dominant Shpol'skii site has been detected in all matrixes and attributed to perylene molecules substitutionally entering the host lattice. The character of the highest-energy site observed in all matrixes was found to be strongly dependent on the nature of solvent. Three matrixes were selected for a comparative study: *n*-hexane, forming a "good" matrix, and *n*-decane and *n*-undecane, forming "poor" matrixes. A vibrational analysis of all Shpol'skii sites was performed, and an additional low-frequency out-of-plane vibration at ca. 190 $cm^{-1}$ was observed for the highest energy site in *n*-decane and *n*-undecane matrixes in highly resolved two-dimensional spectra. Vibrational frequencies detected in "conventional" emission and excitation spectra and in two-dimensional spectra, as well as data from infrared and Raman spectra, are in a good agreement with recalculated vibrational frequencies obtained by MNDO and ab initio quantum-chemical methods.

## 1. Introduction

Photophysical properties of perylene have been extensively studied in many laboratories. In particular, low-temperature luminescence spectra of perylene in polycrystalline Shpol'skii matrixes,[1−7] luminescence narrowing and hole-burning spectroscopy of perylene,[8−14] jet-cooled fluorescence spectra of molecules excited to the $S_1$ state,[15−18] and IR and Raman spectra[19−22] were reported. Perylene became a model molecule after it had been established that its solutions can be studied by the modern technique of single-molecule spectroscopy (SMS). The technique of SMS requires that the solute molecules be fixed in a well-defined and geometrically and energetically stable environment to minimize the spectral diffusion and enhance the reproducibility of spectral features. For this reason, crystal lattices of Shpol'skii matrixes come as an obvious choice.

In earlier works on SMS of perylene, the molecule was placed in polyethylene and in *n*-nonane.[23,24] Recently, calculations of properties of the Shpol'skii system perylene in *n*-alkanes were performed using a combination of quantum mechanics and molecular mechanics.[25] The study has recently been extended to a series of other *n*-alkane matrixes, from *n*-hexane to *n*-decane.[26]

Earlier research into Shpol'skii spectra of perylene[26] and terrylene[27] in several *n*-alkane matrixes clearly pointed to an important role of the geometrical compatibility of the solute and solvent molecules. In the previous papers reporting on perylene spectra,[25,26] the matrixes were chosen so as to ensure a good compatibility of the shapes. Experimental results provided in this paper extend the series of solvents to higher *n*-alkanes in which the solute−solvent compatibility can hardly be expected: low-temperature fluorescence and fluorescence excitation spectra of perylene molecule in *n*-decane and *n*-undecane matrixes are reported and compared with the spectra obtained in *n*-hexane. We employed the technique of total luminescence spectroscopy (TLS) described in detail in refs 28−31. TLS was earlier used for a detailed study of properties of aromatic hydrocarbons[27,29−31] and of fullerenes[32] and is of outstanding value if the emission spectra are excitation-wavelength-dependent.[27,29−31]

For the purpose of this paper, we shall first summarize basic features of TLS spectra of molecules in Shpol'skii matrixes. Peak frequencies associated with the presence of a site *i* fulfill the relation

$$\nu_{ex}^{i} = \nu_{em}^{i} + \nu_{vib}(S_0) + \nu_{vib}(S_1)$$

where $\nu_{ex}^{i}$ and $\nu_{em}^{i}$ denote wavenumbers of excitation and emission transitions and $\nu_{vib}(S_0)$ and $\nu_{vib}(S_1)$ are the wavenumbers corresponding to vibration frequencies of the ground and excited states, respectively. It is important to note that $\nu_{vib}(S_0)$ and $\nu_{vib}(S_1)$ do not depend strongly on the specific site. Therefore, multiplet TLS spectra can be described by a weighted superposition of identical single-site vibronic patterns, each subspectrum (*i*) shifted relative to another one (*j*) in the ($\nu_{ex}$,$\nu_{em}$) plane along a diagonal line with the slope ($\{\partial\nu_{ex}\}/\{\partial\nu_{em}\}$) amounting to 1 (see ref 29). This energy shift between two subspectra *i* and *j* amounts to $(\Delta\nu^{ij})/(\sqrt{2})$, where $\Delta\nu^{ij}$ is the respective site splitting. The site splitting $\Delta\nu^{ij}$ between the sites *i* and *j* for a given electronic-vibrational transition is

$$\Delta\nu^{ij} = \nu_{ex}^{i} - \nu_{ex}^{j} = \nu_{em}^{i} - \nu_{em}^{j}$$

Note that, because of strong Rayleigh scattering, observation of resonant 0−0 transitions (i.e., of the origin of the multiplet) is possible only if time-resolved techniques are applied.[33]

In some cases, TLS spectra cannot be regarded as a superposition of identical single-site patterns and contain additional ("off-diagonal") features. Such features can be attributed either to the presence of impurities (e.g., products of

* To whom correspondence should be addressed. Fax: +48 71 320 3364. E-mail: palewska@kchf.ch.pwr.wroc.pl.

10.1021/jp020493p CCC: $22.00 
Published on Web 04/17/2002

**TABLE 1: Calculated Bond Lengths (Å) of Perylene in Ground and the First Singlet States (Results of MNDO and ab Initio 6-31G* Calculations Compared to Mean Measured Values)**

| distance type[a] | observed distance[b] | calculated (MNDO method) distance | | | calculated (ab initio method) distance | | |
|---|---|---|---|---|---|---|---|
| | | $S_0$ state | $S_1$ state | $\Delta(S_1-S_0)$ | $S_0$ state | $S_1$ state | $\Delta(S_1-S_0)$ |
| a | 1.371 | 1.379 | 1.392 | +0.013 | 1.356 | 1.382 | +0.026 |
| b | 1.418 | 1.424 | 1.408 | −0.016 | 1.407 | 1.379 | −0.028 |
| c | 1.397 | 1.397 | 1.424 | +0.027 | 1.370 | 1.416 | +0.046 |
| d | 1.425 | 1.453 | 1.446 | −0.007 | 1.430 | 1.419 | −0.011 |
| e | 1.424 | 1.436 | 1.447 | +0.011 | 1.414 | 1.431 | +0.017 |
| f | 1.400 | 1.437 | 1.430 | −0.007 | 1.416 | 1.406 | −0.010 |
| g | 1.471 | 1.481 | 1.460 | −0.021 | 1.485 | 1.441 | −0.044 |

[a] Symbols corresponding to those used in Figure 1a. [b] Averaged values taken from ref 38.

photochemical reactions[34]) or to differences in geometry of the guest molecules in their ground and excited states[30] or, finally, to the presence of molecules incorporated into highly disordered ("pseudoliquid") regions of the matrixes.[5,27] The TLS spectra immediately point to the existence of such features.

## 2. Experimental Methods and Quantum-Chemical Calculations

Spectroscopic measurements were carried out on a computer-controlled system consisting of two double-grating SPEX 1402 monochromators.[28] The excitation monochromator was equipped with an Osram XBO 2500 W xenon arc as light source. A Hamamatsu R2949 photomultiplier in photon-counting mode was mounted to the emission monochromator to detect the dispersed fluorescence. The two-dimensional spectra were measured by sequentially recording emission spectra at various excitation frequencies. The spectral resolution for TLS measurements was greater than $\pm 15$ cm$^{-1}$.

High-quality zone-refined perylene was obtained from Prof. Norbert Karl (3. Physikalisches Institut, Universität Stuttgart). The solvents employed in the present study were purchased from Fluka in purum or puriss grade quality; their purities were checked chromatographically. The concentrations of perylene in the solutions under study ranged from $1.8 \times 10^{-7}$ M in *n*-hexane to $4 \times 10^{-7}$ M in *n*-dodecane. Degassed perylene solutions were placed in an Oxford CF204 cryostat, which was precooled to 25 K, and polycrystalline samples thus obtained were then cooled slowly to a final temperature between 4.2 and 5.0 K, at which the spectra were recorded.

IR spectra of perylene in KBr pellets and in Nujol (below 400 cm$^{-1}$), as well as a Raman spectrum (with $\lambda_{ex} = 632.8$ nm), were recorded with Perkin-Elmer System 2000 FTIR and Jobin Yvon T64000 spectrometers, respectively.

The MNDO method[35] and ab initio Hartree−Fock/6-31 G*[36] calculations using the Gaussian 98[37] package were employed to calculate the optimized ground-state geometry (see Table 1), the force constants, and the harmonic vibrational frequencies of the perylene molecule. The optimized first excited singlet state geometry has been obtained via the CIS procedure implemented in Gaussian. The molecule was assumed to lie in the *x*,*y* plane with its long axis parallel to the *y* direction. The calculated IR frequencies (see Table 3) were scaled by the factor 0.95.

## 3. Results

The fluorescence and fluorescence excitation spectra in *n*-hexane, *n*-decane, and *n*-undecane shown in Figure 2 are representative of fluorescence and fluorescence excitation spectra of perylene in "good" and "poor" *n*-alkane matrixes used in this study. All spectra exhibit multiplet structures; within an experimental error, we observed a resonance agreement between

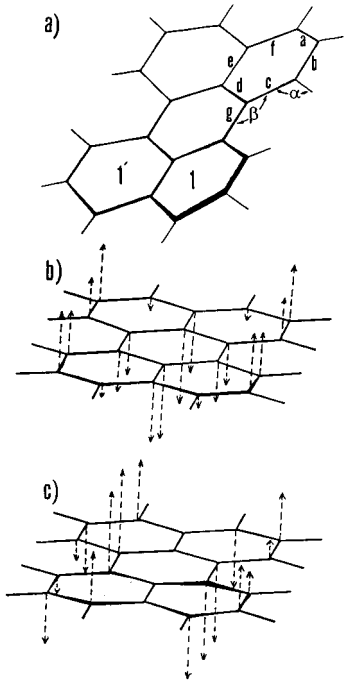


**Figure 1.** Perspective drawing of a perylene molecule (a) in the α modification of the crystal (after ref 39). The bending of the molecule was grossly exaggerated for clarity. Panel b shows an illustration of the lowest butterfly skeletal vibration at 184 cm$^{-1}$ ($B_{1g}$ symmetry) in peryelne; panel c shows the out-of-plane skeletal vibrational mode at 455 cm$^{-1}$ ($B_{2g}$ symmetry). Vibrational modes were calculated using the ab initio method.

the most intense excitation and emission lines. The mirror symmetry between the vibronic patterns in the emission and excitation spectra over the spectral region covered by our experiment is excellent in *n*-hexane and a little worse in *n*-decane and *n*-undecane matrixes (in the latter case, the differences appeared in the intensities of the vibronic lines in the fluorescence and fluorescence excitation spectra). The structure of the 0−0 region of the $S_1 \leftrightarrow S_0$ transition was found to be sensitive to the nature of the matrix: the best-resolved multiplet spectra have been observed in *n*-hexane. In the fluorescence spectrum (Figure 2a), the components of the multiplet appear at 22 413 cm$^{-1}$ ($0_B$, a very strong line) and at 22 474 and 22 538 cm$^{-1}$ (weaker components labeled $0_C$ and $0_D$, respectively). Additionally, a fourth very weak component at 22 757 cm$^{-1}$ ($0_A$) was found (see insert in Figure 2a). In the fluorescence excitation spectrum, we observed only a very strong line at 22 418 cm$^{-1}$, corresponding to the $0_B$ component (the other ones are hidden under the phonon wing following the $0_B$ line).

The fluorescence spectrum of perylene in the *n*-decane matrix consists of two lines at 22 525 cm$^{-1}$ ($0_B$) and 22 740 cm$^{-1}$ ($0_A$) and of a broad band peaking at about 22 625 cm$^{-1}$ associated

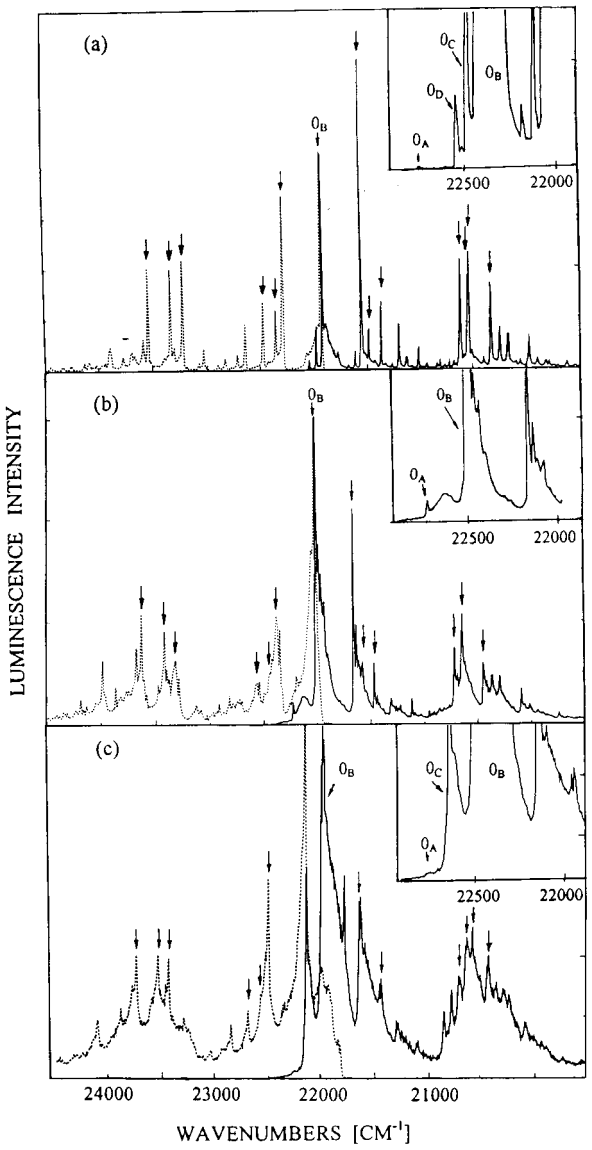


**Figure 2.** Fluorescence emission and excitation spectra of perylene at 5 K in (a) *n*-hexane ($c = 1.8 \times 10^{-7}$ M), (b) *n*-decane ($c = 3 \times 10^{-7}$ M), and (c) *n*-undecane ($c = 4 \times 10^{-7}$ M). Full lines represent fluorescence spectra excited at 23 810 ± 45 cm$^{-1}$ in all matrixes; dashed lines represent excitation spectra monitored in *n*-hexane at 21 100 ± 35 cm$^{-1}$, in *n*-decane at 22 150 ± 35 cm$^{-1}$, and in *n*-undecane at 21 050 ± 35 cm$^{-1}$. All lines corresponding to fundamental frequencies of the B site (cf. Table 3) are marked with arrows. Inserts show the 0−0 regions of the fluorescence spectra.

with the 0−0 of the $S_1 \rightarrow S_0$ transitions. In the fluorescence excitation spectrum, only a strong line at 22 518 cm$^{-1}$ belonging to the $0_B$ component has been observed.

Two dominant lines, associated with the 0−0 transition, were found in the fluorescence spectrum of perylene in the *n*-undecane matrix at 22 503 cm$^{-1}$ ($0_B$) and at 22 635 cm$^{-1}$ ($0_C$). Additionally, a very weak third component at 22 762 cm$^{-1}$ ($0_A$) was found (see insert in Figure 2c). In the excitation spectrum, we observed a strong line at 22 640 cm$^{-1}$, corresponding to the $0_C$ component and a second component at 22 508 cm$^{-1}$ corresponding to the $0_B$ site. The 0−0 fluorescence and fluorescence excitation lines detected in spectra of perylene in all matrixes used in this study are listed in Table 2.

The TLS spectra of perylene in all *n*-alkane matrixes used in this study are shown in Figure 3a−c. These figures cover approximately the $\nu_{00} + 1300$ cm$^{-1}$ region in excitation and

**TABLE 2: Multiplets of the 0−0 Transitions in the Fluorescence and Fluorescence Excitation Spectra of the Perylene Molecule in Various Hydrocarbon Matrixes at 5 K (in cm$^{-1}$)**

| | transitions[a] | |
|---|---|---|
| matrix | $S_1 \rightarrow S_0$ | $S_1 \leftarrow S_0$ |
| *n*-hexane | 22 413 v s ($0_B$) | 22 418 v s |
| | 22 474 w ($0_C$) | |
| | 22 538 w ($0_D$) | |
| | 22 757 v w ($0_A$) | |
| *n*-decane | 22 525 v s ($0_B$) | 22 518 v s |
| | 22 740 w ($0_A$) | |
| *n*-undecane | 22 503 v s ($0_B$) | 22 508 m |
| | 22 635 s ($0_C$) | 22 640 s |
| | 22 762 w ($0_A$) | |

[a] Abbreviations: w = weak; m = medium; s = strong; v = very.

$\nu_{00} - 1500$ cm$^{-1}$ region in fluorescence. Maxima associated with vibrational frequencies of the solute molecule occupying a few sites are visible on the maps and isometric plots. In the following, the discussion will be focused on features associated with the lowest-frequency skeletal vibrations, in which the effect of the matrix in best visible.

In all solvents, perylene molecules occupy one strongly dominant and well-defined site (labeled B, see Table 2 and Figure 3). The inhomogeneous broadening of the line in *n*-hexane is relatively small (fwhm ≅ 25 cm$^{-1}$), as are the widths of the cross sections of the phonon wing, both in emission and excitation. In *n*-decane and *n*-undecane, the inhomogeneous broadening is considerably bigger, and the lines located on the diagonals—$\nu_{ex} = \nu_{em} + 349$ cm$^{-1}$, $\nu_{ex} = \nu_{em} + 432$ cm$^{-1}$ and $\nu_{ex} = \nu_{em} + 347$ cm$^{-1}$, $\nu_{ex} = \nu_{em} + 430$ cm$^{-1}$ in *n*-decane and *n*-undecane, respectively—are hard to resolve (contrary to perylene in the *n*-hexane matrix). The second component observed in the 0−0 of the $S_1 \leftrightarrow S_0$ transition (labeled A) appears clearly in the two-dimensional spectra (the location of the site A is marked in Figure 3). It should be noted that the energy of the purely electronic $S_1 \leftrightarrow S_0$ transition for this site is over 200 cm$^{-1}$ higher than the respective energy for the most prominent B site. Moreover, as can be verified upon inspection of the spectra displayed in Figure 3, the shapes of the lines associated with the site A are strongly dependent on the nature of the solvent: the best Shpol'skii effect is observed in *n*-hexane. Cross sections of the 2D spectra of perylene in *n*-decane and *n*-undecane taken at constant emission wavenumbers corresponding to the site A ($\nu_{em} = 22\,740$ cm$^{-1}$ and $\nu_{em} = 22\,762$ cm$^{-1}$, respectively) allow one to identify additional lines belonging to the site A and located on the diagonals, $\nu_{ex} = \nu_{em} + 193 \pm 7$ cm$^{-1}$ and $\nu_{ex} = \nu_{em} + 186 \pm 7$ cm$^{-1}$, respectively. Simultaneously, two other lines detected for the remaining sites (at ca. 348 and 431 cm$^{-1}$, see above) have not been observed among the lines belonging to the site A. The peak at ca. 190 cm$^{-1}$ should also be observed in cross sections of the 2D spectra taken at constant excitation wavenumbers. Unfortunately, this feature has not been observed, being probably hidden under a very intense phonon wing of the 0−0 transition of the site B.

Apart from the main doublet (A and B), a third component of the Shpol'skii multiplet (labeled C) is observed in *n*-undecane, as well as in all matrixes used in ref 26 except *n*-decane (see Table 2). In *n*-decane, features associated with this site spread into a distribution that additionally overlaps with features due to the inhomogeneous broadening of the line belonging to the site B. A fourth component, weak but distinct (labeled D), is clearly visible only in the *n*-hexane matrix, in other matrixes being probably hidden under the tails of B and C sites. Moreover, there exists a distribution of red-shifted sites (labeled

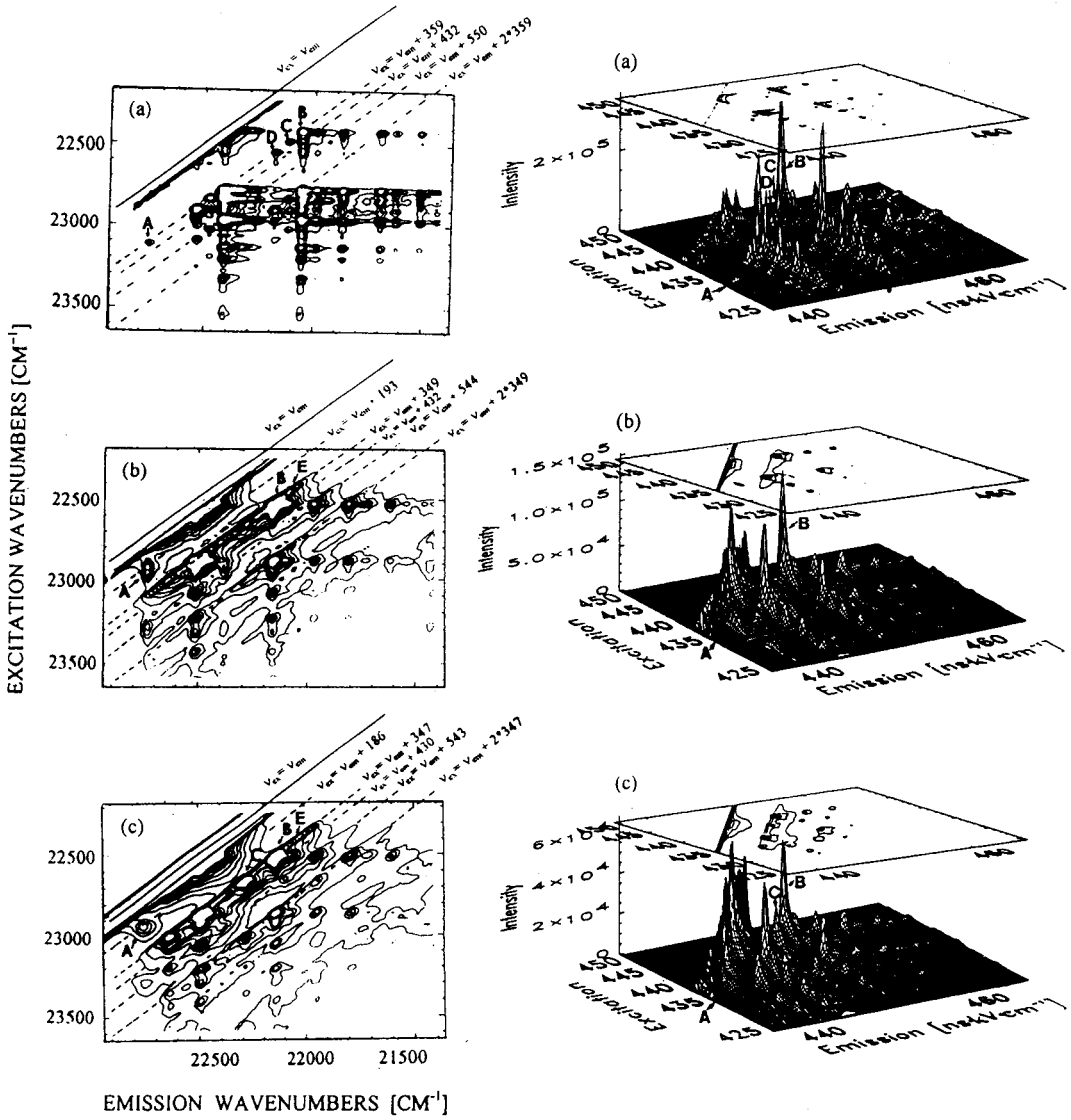


**Figure 3.** Contour and isometric plots of TLS high-resolved Shpol'skii spectra of perylene in *n*-alkane matrixes at 5 K. The capital letters indicate sites as described in the text. The solvents and concentrations (at room temperature) are (a) *n*-hexane at $c = 1.8 \times 10^{-7}$ M, (b) *n*-decane at $c = 3 \times 10^{-7}$ M, and (c) *n*-undecane at $c = 4 \times 10^{-7}$ M. All spectra have been cut at the 1% intensity level to show weaker sites.

**TABLE 3: Fundamental Vibrational Frequencies (in cm$^{-1}$) of Perylene Identified in the Fluorescence and Fluorescence Excitation Spectra in Some *n*-Alkane Matrixes[a] at 5 K and IR and Raman Frequencies Identified at Room Temperature Compared with Results of Quantum-Chemical Calculations**

| excitation[b] | | fluorescence[b] | | | | description of vibration | |
|---|---|---|---|---|---|---|---|
| *n*-hexane | *n*-decane | *n*-hexane | *n*-decane | IR[b] | Raman[b] | ref 39 | present calculations (ab initio) |
| | 193 s[c] | | | 184 m | 189 w | 176 $B_{2g}$ (out-of-plane) | 184 $B_{1g}$ (out-of-plane) |
| 359 s | 356 s | 358 s | 349 s | | 361 m | 364 $A_g$ (in-plane) | 360 $A_g$ (in-plane) |
| 426 m | 432 w | 432 w | 423 w | | 446 w | 430 $B_{1g}$ (out-of-plane) | 455 $B_{2g}$ (out-of-plane) |
| 547 m | 552 m[d] | 550 m. | 544 m | 540 m | 547 m | 548 $A_g$ (in-plane) | 553 $A_g$ (in-plane) |
| 1294 s | 1294 m | 1302 s | 1292 m | 1288 m | 1296 s | 1299 $A_g$ (in-plane) | 1275 $A_g$ (in-plane) |
| | | 1372 s | 1369 m | | 1370 v s | 1369 $A_g$ (in-plane) | 1370 $A_g$ (in-plane) |
| 1407 s | 1403 m | 1382 s | | 1380 m | 1396 v w | 1373 $A_g$ (in-plane) | 1387 $A_g$ (in-plane) |
| 1614 s | 1615 m | 1574 s | 1569 m | | 1569 v s 1577 w | 1568 $A_g$ (in-plane) | 1543 $A_g$ 1607 $A_g$ (in-plane) |

[a] The values given in the table were determined from the analysis of the lines belonging to the "B" site. [b] Abbreviations: w = weak; m = medium; s = strong; v = very. [c] The frequency observed in 2D spectra belonging only to the "A" site. [d] The frequency observed in 2D spectra belonging to both "A" and "B" sites.

E) manifesting itself as a tail on the diagonals, $\nu_{ex} = \nu_{em} + 349 \pm 7$ cm$^{-1}$ and $\nu_{ex} = \nu_{em} + 347 \pm 7$ cm$^{-1}$ in *n*-decane and *n*-undecane, respectively (cf. Figure 3b,c). The pattern corresponding to the distribution is quite intense in these two matrixes, being almost absent in shorter *n*-hexane.

Fundamental vibration frequencies of perylene in the $S_0$ and $S_1$ states, determined from the analysis of the emission and excitation spectra, are given in Table 3. The table also contains corresponding vibrational frequencies observed in IR and Raman spectra, compared with frequencies determined by Cyvin et al.[39] The frequencies are also in a good agreement with those identified in highly resolved electronic−vibronic spectra by Personov et al.,[3,4] as well as with the frequencies observed in IR and Raman spectra by Cyvin et al.[39] It should also be noted

that the low-frequency out-of-plane vibration identified in our 2D spectra of perylene (193 $cm^{-1}$ in *n*-decane and 186 $cm^{-1}$ in *n*-undecane) has also been found in the IR and Raman spectra (cf. Table 3). The existence of an intense out-of-plane butterfly ($B_{1g}$ symmetry) vibronic transition at 184 $cm^{-1}$, both in the ground and in the excited states, has also been confirmed by the quantum-chemical calculations (cf. Figure 1b). Apart from the 184 $cm^{-1}$ vibration, there exists another out-of-plane vibration ($B_{2g}$ symmetry) at 455 $cm^{-1}$ (Figure 1c), the presence of which has been confirmed in all excitation and emission spectra (cf. Table 3).

The structure of the perylene molecule as determined from X-ray experiments performed on single crystals is shown in Figure 1a. Quantum-chemical calculations performed for the isolated perylene molecule showed that in the ground state the molecule is planar whereas its shape slightly deviates from planarity in the $S_1$ state (the deviation amounts to ca. 0.04°). The calculated peri bond lengths linking two naphthalene units (labeled g in Figure 1a) are the longest bonds in both the ground and excited states of perylene molecule, and all bond lengths of the central ring of the perylene molecule become considerably shorter in the first excited singlet state. Simultaneously, the calculated values of the $\alpha$ and $\beta$ angles decrease in the $S_1$ state by no less than 0.2°. A small but significant deviation from a completely planar arrangement also was observed in $\alpha$-perylene crystals.[38] The dihedral angle between 1 and 1′ naphthalene rings (see Figure 1a) was evaluated to be 178.7° (the deviation from the mean plane was found to be about $10^{-3}$ Å).

## 4. Discussion and Conclusions

The experiments reported in the present paper demonstrate that the guest perylene molecules occupy at least four well-defined sites, differing in the geometry of the environment of the emitting molecules. The site labeled B is most well-defined and appears in all matrixes used in the research reported here. The shape of the TLS line attributed to the B site is due to a small width of the zero-phonon line, that is, to a relatively small inhomogeneous broadening. This indicates that the guest molecules enter the host lattice in a well-defined manner. We can conclude, in agreement with results of earlier calculations,[26] that B sites are formed by perylene substitutionally replacing the solute molecules and have a minimal freedom.

As was mentioned in the preceding section, the shapes of the lines associated with the site B are different from those associated with the site A. In particular, the high intensity of the phonon wing in the latter site may point to an efficient electron−phonon coupling much stronger than that in the site B. This seems to indicate that the arrangement of the host molecules in this site is not strictly defined or the perylene molecules enjoy some freedom of orientation, or both. Moreover, a comparison of the energy of the purely electronic $S_1 \leftrightarrow S_0$ transition determined for gaseous perylene (24 070 $cm^{-1}$ in ref 40) with the respective energies of the A and B sites (ca. 22 750 $cm^{-1}$ and ca. 22 500 $cm^{-1}$ depending on the solvent, cf. Table 2) seems to point to weaker interactions between the solute molecules and the matrixes in the A site. One may thus speculate that in the A site the guest molecules would be located on a defect, sufficiently well-defined yet providing a distribution of environments and hence a distribution of energies of solute−solvent interactions. The same may also be true for the less-populated sites C and D (the C site was found in almost all studied *n*-alkane matrixes,[25,26] whereas the D site is clearly visible only in *n*-hexane).

The main conclusion that may be drawn on the basis of the results reported in this paper is a further confirmation of the principle of the best geometric compatibility between the dimensions on the solute and solvent molecules.[27] A straightforward comparison of the molecular dimensions of perylene and of the *n*-alkanes used allows one to predict that the solute molecules will best fit into the *n*-hexane or *n*-octane matrixes. Indeed, the results presented in this paper confirm that *n*-hexane forms a "good" matrix for perylene. The conclusion is also confirmed by results obtained for perylene in other *n*-alkane matrixes.[26]

The fundamental frequencies are given in Table 3 and are indicated by the arrows in Figure 2. Furthermore, overtones of the strongest vibronic frequencies, as well as combinations with all other vibrations, are also visible in the spectra. The most intense line in the fluorescence spectra of the B site appearing in all solvents at 352 ± 7 $cm^{-1}$ below the 0−0 transition is in a very good agreement with the results of other authors (e.g., refs 1−7). In the excitation spectra, the strongest line appears at nearly the same frequency above the 0−0 transition.

In the TLS spectra of perylene in some matrixes, we have observed a feature associated with a low-frequency vibration (ca. 190 $cm^{-1}$). This frequency, previously detected in IR and Raman spectra of perylene (ref 41, see also Table 3) and attributed to out-of-plane vibration of the molecule,[39] has not been detected in the "conventional" excitation spectra; moreover, in 2D spectra it could only be observed in "poor" matrixes (*n*-decane ane *n*-undecane). We attribute this feature to the fact that the low-frequency vibration is of the butterfly character, thus being space-demanding and possible only in matrixes in which, because of misfit, the solute molecules enjoy a considerable freedom of motions.

It should be stressed that the IR and Raman experiments were performed on samples containing perylene crystallites. Perylene molecules are known to be nonplanar in the crystals,[38] whereas both experiment[42,43] and quantum-chemical calculations (see the preceding section) show that isolated perylene molecules are planar. Thus, the appearance of the low frequency in the 2D spectra is likely to be related to a change of the geometry of the solute molecules in A sites. Any more farther-reaching conclusions concerning this point cannot, however, be drawn on the basis of the experiments described in this paper.

**Acknowledgment.** The emission spectra reported in this paper were recorded at the Physical Chemistry Laboratory, Swiss Federal Institute of Technology (ETH Zurich). K.P. is grateful to Professor Urs P. Wild for his hospitality and help. Thanks are also due to Professor N. Karl for the gift of high-purity perylene used in the present study. The work was supported by the Swiss National Science Foundation and by the Technical University of Wrocław.

## References and Notes

(1) Personov, R. I. *Izv. Akad. Nauk SSSR, Ser. Fiz.* **1960**, *24*, 620 (in Russian).
(2) Al'shits, E. I.; Godyaev, E. D.; Personov, R. I. *Fiz. Tverd. Tela* **1972**, *14*, 1605 (in Russian).
(3) Shpol'skii, E. W.; Personov, R. I. *Opt. Spectrosc.* **1960**, *8*, 328 (in Russian).
(4) Val'dman, M. M.; Personov, R. I. *Opt. Spectrosc.* **1965**, *19*, 531 (in Russian).
(5) Pfister, C. *Chem. Phys.* **1973**, *2*, 171; **1973**, *2*, 181.
(6) Lamotte, M.; Merle, A. M.; Joussot-Dubien, J.; Dupuy, F. *Chem. Phys. Lett.* **1975**, *35*, 410.
(7) Lamotte, M.; Joussot-Dubien, J. *J. Chem. Phys.* **1974**, *61*, 1892.
(8) Al'shits, E. I.; Kharlamov, B. M.; Personov, R. I. *Opt. Spectrosc.* **1988**, *65*, 548 (in Russian).
(9) Personov, R. I. *J. Photochem. Photobiol., A: Chem.* **1992**, *62*, 321.
(10) Orrit, M.; Bernard, J.; Personov, R. I. *J. Phys. Chem.* **1993**, *97*, 10256.

(11) Personov, R. I.; Kharlamov, B. M. *Opt. Commun*. **1973**, *7*, 417.
(12) Abram, I. I.; Auerbach, R. A.; Birge, R. R.; Kohler, B. E.; Stevenson, J. M. *J. Chem. Phys.* **1975**, *63*, 2473.
(13) Hurst, G. B.; Wright, J. C. *J. Chem. Phys.* **1991**, *95*, 1479.
(14) Personov, R. I.; Al'shits, E. J.; Bykovskaya, L. A. *Opt. Commun*. **1972**, *6*, 169.
(15) Fourmann, B.; Jouvet, C.; Tramer, A.; Le Bars, J. M.; Millié, Ph. *Chem. Phys.* **1985**, *92*, 25.
(16) Bouzou, C.; Jouvet, C.; Leblond, J. B.; Millié, Ph.; Tramer, A.; Sulkes, M. *Chem. Phys. Lett.* **1983**, *97*, 161.
(17) Schwartz, S. A.; Topp, M. R. *Chem. Phys.* **1984**, *86*, 245.
(18) Fillaux, F. *Chem. Phys. Lett.* **1985**, *114*, 384.
(19) Ambrosino, F.; Califano, S. *Spectrochim. Acta* **1965**, *21*, 1401.
(20) Babkov, L. M.; Kovner, M. A.; Rents, V. B. *Opt. Spectrosc*. **1972**, *34*, 615 (in Russian).
(21) Maddams, W. F.; Royaud, I. A. M. *Spectrochim. Acta* **1990**, *46A*, 309.
(22) Szczepanski, J.; Chapo, Ch.; Vala, M. *Chem. Phys. Lett.* **1993**, *205*, 434.
(23) Basché, Th.; Moerner, E. W. *Nature* **1992**, *355*, 335.
(24) Pirotta, M.; Renn, A.; Werst, M. H. V.; Wild, U. P. *Chem. Phys. Lett.* **1996**, *250*, 576.
(25) Wallenborn, E.-U.; Leontidis, E.; Palewska, K.; Suter, U. W.; Wild, U. P. *J. Chem. Phys.* **2000**, *112*, 1995.
(26) Leontidis, E.; Heinz, H.; Palewska, K.; Wallenborn, E.-U.; Suter, U. W. *J. Chem. Phys*. **2001**, *114*, 3224.
(27) Palewska, K.; Lipiński, J.; Sworakowski, J.; Sepioł, J.; Gygax, H.; Meister, E. C.; Wild, U. P. *J. Phys. Chem*. **1995**, *99*, 16835.
(28) Suter, G. W.; Kallir, A. J.; Wild, U. P. *Chimia* **1983**, *37*, 413.
(29) Kallir, A. J.; Suter, G. W.; Bucher, S. E.; Meister, E. C.; Lüönd, M.; Wild, U. P. *Acta Phys. Pol.* **1987**, *A71*, 755.
(30) Palewska, K.; Meister, E. C.; Wild, U. P. *Chem. Phys*. **1989**, *138*, 115.
(31) Palewska, K.; Meister, E. C.; Wild, U. P. *J. Lumin*. **1991**, *50*, 47.
(32) Palewska, K.; Sworakowski, J.; Chojnacki, H.; Meister, E. C.; Wild, U. P. *J. Phys. Chem*. **1993**, *97*, 12167.
(33) Meister, E.C. Ph.D. Thesis, ETH Zurich, Zurich, Switzerland, 1988.
(34) Palewska, K.; Meister, E. C.; Wild, U. P. *J. Photochem. Photobiol. A: Chem*. **1989**, *50*, 239.
(35) Dewar, M. J. S.; Thiel, W. *J. Am. Chem. Soc*. **1977**, *99*, 4899.
(36) Hariharan, P. C.; Pople, J. A. *Theor. Chim. Acta* **1973**, *28*, 213.
(37) Frisch, M. J.; Trucks, G. W.; Schlegel, H. B.; Scuseria, G. E.; Robb, M. A.; Cheeseman, J. R.; Zakrzewski, V. G.; Montgomery, J. A., Jr.; Stratmann, R. E.; Burant, J. C.; Dapprich, S.; Millam, J. M.; Daniels, A. D.; Kudin, K. N.; Strain, M. C.; Farkas, O.; Tomasi, J.; Barone, V.; Cossi, M.; Cammi, R.; Mennucci, B.; Pomelli, C.; Adamo, C.; Clifford, S.; Ochterski, J.; Petersson, G. A.; Ayala, P. Y.; Cui, Q.; Morokuma, K.; Malick, D. K.; Rabuck, A. D.; Raghavachari, K.; Foresman, J. B.; Cioslowski, J.; Ortiz, J. V.; Stefanov, B. B.; Liu, G.; Liashenko, A.; Piskorz, P.; Komaromi, I.; Gomperts, R.; Martin, R. L.; Fox, D. J.; Keith, T.; Al-Laham, M. A.; Peng, C. Y.; Nanayakkara, A.; Gonzalez, C.; Challacombe, M.; Gill, P. M. W.; Johnson, B. G.; Chen, W.; Wong, M. W.; Andres, J. L.; Head-Gordon, M.; Replogle, E. S.; Pople, J. A. *Gaussian 98*, revision A.1; Gaussian, Inc.: Pittsburgh, PA, 1998.
(38) Camerman, A.; Trotter, J. *Proc. R. Soc. London, Ser. A* **1964**, *279*, 129.
(39) Cyvin, S. J.; Cyvin, B. N.; Klaeboe, P. *Spectrosc. Lett.* **1983**, *16*, 239.
(40) Sonnenschein, M.; Amirav, A.; Jortner, J. *J. Phys. Chem.* **1984**, *88*, 4214.
(41) Palewska, K. Unpublished results.
(42) Traetteberg, M. *Proc. R. Soc. London, Ser. A* **1965**, *283*, 557.
(43) Dallinga, G.; Toneman, L. H.; Traettenberg, M. *Recl. Trav. Chim. Pays*−*Bas* **1967**, *86*, 795.